Chinese Chemical Letters 33 (2022) 1936–1940

Contents lists available at ScienceDirect

Chinese Chemical Letters

journal homepage: www.elsevier.com/locate/cclet

Short and simple peptide-based pH-sensitive hydrogel for antitumor drug delivery

Jie Li[a,1], Zhongshi Wang[a,b,1], Han Han[b], Zhonghua Xu[a], Shasha Li[c], Ying Zhu[b], Yuejian Chen[d], Liang Ge[b,c], Yuan Zhang[a,*]

[a] Department of Orthopedics, Xinqiao Hospital, Army Medical University, Chongqing 400038, China
[b] State Key Laboratory of Natural Medicines, China Pharmaceutical University, Nanjing 210009, China
[c] School of Pharmacy, Xinjiang Medical University, Urumqi 830054, China
[d] Nanjing aifarui Pharmaceutical Technology Co., Ltd., Nanjing 210009, China

ARTICLE INFO

Article history:
Received 29 July 2021
Revised 16 October 2021
Accepted 19 October 2021
Available online 29 October 2021

Keywords:
Peptide hydrogel
pH Sensitivity
Antitumor
Drug delivery
Targeted therapy

ABSTRACT

Since self-assembled peptide hydrogels can solve the problems such as low solubility, poor selectivity and serious adverse effects of traditional chemotherapy drugs, they have been widely used as carrier materials for drug delivery. In this study, we developed a novel and injectable drug delivery platform for the antitumor drug doxorubicin (DOX) using a pH-responsive ionic-complementary octapeptide FOE. This octapeptide could self-assemble into stable hydrogel under neutral conditions, while disassemble under the tumor microenvironment. Especially, at pH 5.8, its micromorphology displayed a transition from nanofibers to nanospheres with the change of secondary structure, which enhanced cellular uptake of DOX. In addition, FOE hydrogel serves as a smart drug reservoir by localized injection to achieve sustained drug release and improve antitumor efficacy. This octapeptide opens up new avenues for promoting the clinical translation of anticancer drugs on account of excellent injectable properties and economic benefits of simple and short sequence.

Cancer is the leading cause of the increasingly mortality worldwide. Chemotherapy is one of the most commonly used treatments for cancer [1]. Among all the anticancer chemotherapy drugs, the small molecular chemotherapy drugs such as DOX are the most classic and prevalent. However, the clinical application of them has been limited due to its low solubility, poor target specificity, large side effects and short biological half-life [2–4]. To address these issues, a variety of polymer nano-carriers such as nanoparticles, liposomes and micelles have been designed, but they still have following limitations: low drug loading capacity, poor biocompatibility and low selectivity toward tumor tissue [5–7]. Accordingly, there is an urgent need to develop novel drug delivery systems (DDSs) to deliver anticancer drugs efficiently.

Hydrogels are defined as three-dimensional hydrophilic polymer networks which could absorb water and then swell in aqueous solution [8]. Several researches have revealed that hydrogels play a major role in biomedical applications, such as tissue engineering, vaccine preparations and drug delivery carriers, due to their tunable physicochemical properties [6,9,10]. Especially, localized drugs delivery using injectable hydrogels has attracted more interests since it could provide a sustained release of drugs at the target site [11,12]. Peptides, important structural elements of the hydrogel networks, possess remarkable properties of low immunogenicity, versatile functionality, as well as inherent biocompatibility and biodegradability [13–15]. Self-assembled peptides can spontaneously organize into well-ordered nanostructures via hydrogen bonding, π-π stacking, electrostatic and hydrophobic interactions [16]. Furthermore, due to the diversity in amino acid side chains, self-assembled peptides with specific secondary structures and properties could be designed by changing their sequence [17–19]. For instance, Webber *et al.* reported a peptide amphiphile (KRRASVAGK[C_{12}]-NH_2) containing the specific consensus substrate for protein kinase A to achieve targeted drug release at the tumor site [20]. Liang *et al.* also proposed a peptide amphiphile-based DDS consisting of mimicking peptide (DRQI KIWF QNRR MKWKK) and stearic acid, which exhibits the advantage of pH-induced conformational/structural transition to release antitumor drugs specifically into tumor cell [21]. More intriguingly, peptide-based hydrogels can change their properties upon external stimuli, such as temperature, pH, enzyme, so as to accumulate drugs in specific ar-

* Corresponding author.
E-mail address: zhangyuan@tmmu.edu.cn (Y. Zhang).
[1] These authors contributed equally to this work.

https://doi.org/10.1016/j.cclet.2021.10.058
1001-8417/

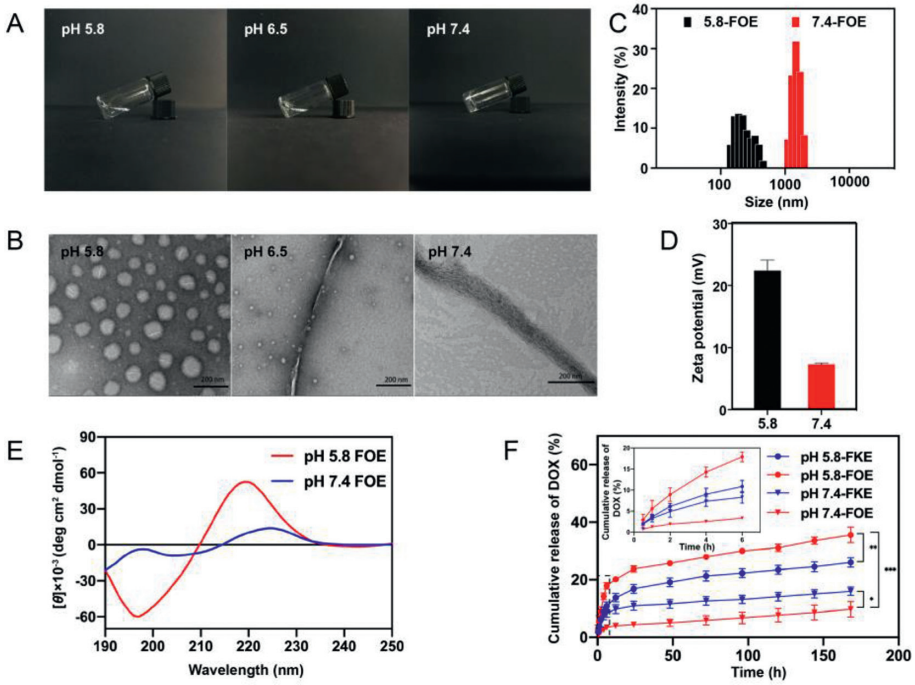

Fig. 1. Characterization of FOE octapeptide under different pH conditions. (A) Appearance of FOE solution (15 mg/mL); (B) TEM images of blank FOE hydrogel (0.10 wt%), scale bar: 200 nm; (C) Dynamic light scattering (DLS) and (D) zeta potential curves of FOE hydrogels; (E) CD spectrum of blank FOE; (F) Cumulative release of DOX from FKE and FOE hydrogels. One-way ANOVA, mean ± SD, $^{*}P$ <0.05, ** P <0.01 and *** P < 0.001, n = 3.

eas [22,23]. Regardless of the remarkable progress, self-assembled peptides are still facing the difficulty that cannot form the stable secondary structure owing to irregular charge and hydrophobicity distribution of their sequence, thereby failing to improve assembly efficiency and mechanical strength of the hydrogel [24]. For this problem, ionic-complementary peptides consisting of alternating hydrophilic and hydrophobic amino acids have attracted extensive attention recently. Their self-assembly is mainly regulated by intermolecular hydrophobic interactions and charged residue interactions [25,26]. However, problems such as low purity of the sample and the difficulty of synthesizing large quantities of peptides at a relatively low cost hinder the further application of this type of peptides [27].

To this end, a novel anticancer DDS based on octapeptide FOE (FOFOFRFE) with ionic self-complementarity was designed and DOX-loaded octapeptide hydrogel was prepared for peritumoral administration herein. The octapeptide sequence is composed of alternate hydrophobic (phenylalanine (F)) and hydrophilic (ornithine (O), arginine (R) and glutamic acid (E)) amino acids, which endows the octapeptide with pH-sensitivity. The octapeptide is able to self-assemble into cross-linked β-sheet nanofibers to form hydrogels in aqueous solution *in vitro*. After peritumoral administration, the octapeptide hydrogel disassembles under acidic microenvironment (pH 5.8), accompanied by the change of microstructure from fiber networks to nanospheres, which will enhance the cellular uptake of drugs. *In vitro*, excellent gelation properties, injectability and biocompatibility of FOE hydrogel were confirmed. *In vivo*, FOE-based DDS was verified to be an effective, sustained, and controllable anticancer drug delivery pathway for targeting tumor sites and limiting cytotoxicity to normal cells.

We synthesized FOE and its analogues using a solid phase peptide synthesis technique shown in Fig. S1 (Supporting information). The ultra-performance liquid chromatography (UPLC) chromatograms, peak data, and Mass Spectrometry confirmation of FOE and its analogues are presented in Figs. S2, S3 and Table S1 (Supporting information). The purity of the designed octapeptides was over 98%, as determined by quantitative UPLC analysis.

Several studies were performed to characterize the self-assembly of FOE octapeptide under different pH conditions. It can be seen that FOE octapeptide self-assembled to form a stable hydrogel under neutral conditions, whereas it was still in a solution state under acidic condition (pH 5.8) (Fig. 1A and Fig. S4 in Supporting information). Under slightly acidic conditions (pH 6.5), the solution gradually became a viscous liquid, indicating the transition process from sol to gel. Meanwhile, transmission electron microscope (TEM) images revealed the morphology of FOE peptide at the microscopic levels (Fig. 1B). The microstructure of the octapeptide solution was uniform nanospheres at pH 5.8, and the nanospheres shrank and gathered with each other to form fine fibers when pH increased to 6.5. When the pH continued to rise to 7.4, FOE octapeptide thickened into strands, and formed a fibrous network structure with uniform pores distributed in the network structure, which could be used to encapsulate drugs. These TEM data confirmed that the typical state of FOE octapeptide under neutral and acidic conditions, namely gel and sol, and directly reflected the pH responsiveness of FOE octapeptide, indicating that FOE can self-assemble into hydrogel at pH 7.4, and disintegrate at pH 5.8.

We further studied the size, zeta potentials and secondary structure (Figs. 1C-E) of the self-assembled octapeptide nanostructures. The particle size of FOE solution was 1506.05 ± 12.64 nm, and the zeta potential was 7.31 ± 0.18 mV at pH 7.4, whereas the former reduced to 237.82 ± 5.20 nm and the latter increased to 22.4 ± 1.71 mV at pH 5.8. The most likely explanation was that the side chain of ornithine was protonated and the electrostatic repulsion between the same charges increased when the pH of the solution was lower than its isoelectric point (pI), which caused the electrostatic repulsion between the octapeptides to exceed the hydrophobic interaction, thereby resulting in the disintegration of the hydrogel and the bending of peptide molecular layer. Interestingly, as shown in Fig. S5 (Supporting information), the incorporation

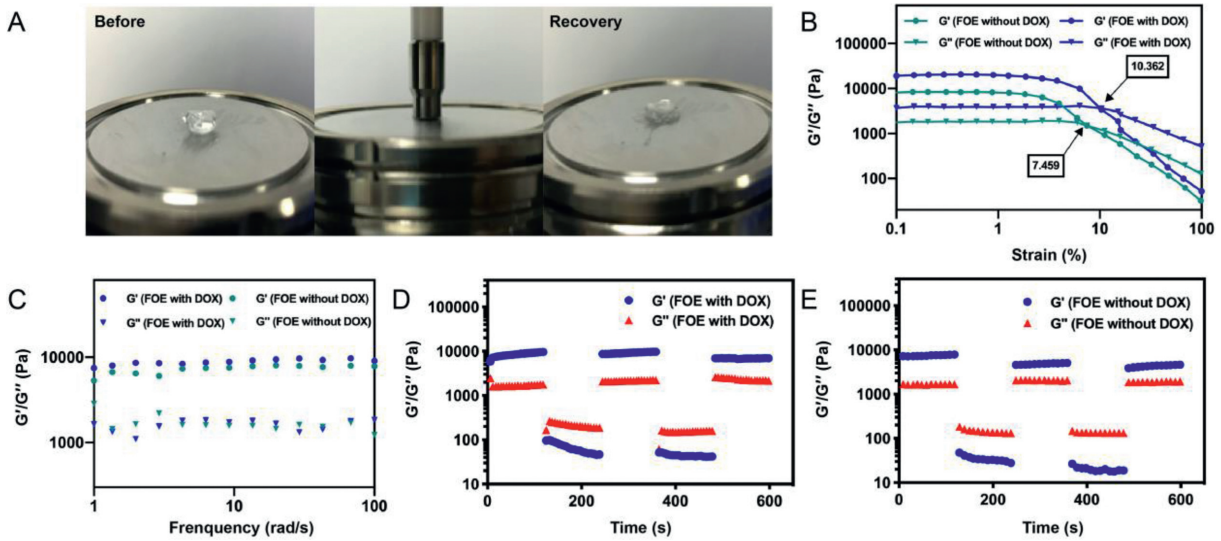

Fig. 2. Rheological study of blank FOE hydrogels and DOX-loaded hydrogels. (A) Photographs of FOE octapeptide during the circle sweep; (B) Dynamic strain sweep of FOE hydrogels with or without DOX; (C) Dynamic frequency scanning of FOE hydrogels with or without DOX; Circle sweep of (D) FOE hydrogels with DOX and (E) FOE hydrogels without DOX.

of DOX led to finer nanofiber networks under neutral conditions. Likewise, the diameter of nanospheres formed by the DOX-loaded FOE was smaller than that of FOE at pH 5.8. A possible reason was that the hydrophobic drug DOX could enhance hydrophobic interaction between the octapeptides, which made the fiber networks denser and the nanospheres smaller [28]. Then, circular dichroism (CD) spectrum was acquired to investigate the secondary structure of FOE octapeptide. The result exhibited that the secondary structure of the peptides varied from random coil at pH 5.8 to coexistence of β-sheet and random coil at pH 7.4, suggesting that FOE octapeptides gradually changed from the solution state to hydrogel at a macroscopic level. This finding corresponds to the change in the appearance of the FOE octapeptide solution, suggesting that FOE peptides have a pH-triggered structural transition.

Subsequently, *in vitro* drug release studies of FOE hydrogel were conducted to verify the pH-responsiveness of FOE hydrogel. We designed the other 2 different octapeptides based on FOE to compare with FOE octapeptide. The basic amino acid ornithine (pI = 10.80) in FOE was replaced with lysine (K, pI = 9.74) to get FKE (FKFKFRFE). And FOR (FOFOFRFR) was designed by replacing glutamic acid with arginine. The gelation properties of these octapeptides were investigated under different conditions. Interestingly, FOR octapeptide cannot self-assemble under the selected conditions (Fig. S6 in Supporting information), possibly due to the fact that hydrophilic amino acids in this octapeptide are all basic amino acids. Thus, the electrostatic repulsion between the same charges is much greater than the hydrophobic force of the amino acid side chains, which was consistent with previous study [29]. Both FKE and FOE could self-assemble at pH 7.4 and form a stable hydrogel, but the gel formation rate of FOE was faster than that of FKE. The reason may be that the side chain of lysine is longer than that of ornithine, causing the larger steric hindrance of self-assembly.

We then compared the drug release properties of FOE hydrogel with that of FKE hydrogel. The cumulative DOX release of FOE hydrogel at pH 5.8 (35.58%) was approximately 3.67-fold higher than that at physiological pH (9.69%) ($P < 0.001$) (Fig. 1F), implying that the FOE octapeptide offered a sustained and pH-induced drug release. In comparison to FKE, cumulative DOX release from FOE hydrogel was less in neutral condition and more in acidic condition, suggesting that the hydrogel formed by FOE had better pH sensitivity and higher stability. This phenomenon may be due to the substitution of basic amino acids (lysine) in FKE by ornithine with a higher pI, making the amino acid side chains more susceptible to pH reduction and easier to protonate. Besides, it was found that there was no drug burst release at the initial phase. The overall results suggested that FOE octapeptide provided much more sustained and efficient drug release.

Rheological tests were performed to characterize the mechanical properties and injectability of FOE hydrogel. The photographs of FOE octapeptide during the cyclic sweep directly showed that even when the gap between the rotor and the sample disk was only 0.5 mm, and the strain was as high as 50%, the hydrogel quickly recovered its morphology after shearing (Fig. 2A), suggesting that FOE formed a stable hydrogel and had good shear-thinning properties. In dynamic strain sweep, both storage modulus (G') and loss modulus (G") of DOX-loaded FOE hydrogel were greater than those of blank FOE hydrogel (Fig. 2B), confirming that the incorporation of DOX reinforced the mechanical strength of FOE hydrogel [28]. We fixed the strain to 1% and performed the dynamic frequency scanning on the sample. It was found that the values of G' dominated those of G", and FOE hydrogel exhibited weak dependence on the frequency ranging from 1 rad/s to 100 rad/s (Fig. 2C), which proved that FOE hydrogel formed a solid-like hydrogel with strong rigidity. In order to study the injectability of FOE hydrogel, cyclic sweep experiment was used to simulate the injection process (Figs. 2D and E). The results demonstrated that FOE hydrogel could recover its structure quickly after repeated destroyed by external force, indicating that FOE peptide was a stable drug carrier that could be dynamically reorganized repeatedly. Consequently, this octapeptide has the potential to be used in the field of biological self-assembly injectable carrier materials.

A MTT assay was used to study the cytotoxicity and biocompatibility of FOE hydrogel to human umbilical vein endothelial cells (HUVECs). The cell viability after co-incubation with blank FOE hydrogel (up to 600 μg/mL) for 48 h was above 95% (Fig. 3A), revealing that FOE has almost no carrier toxicity to normal cells in this concentration range. Then the *in vitro* anti-proliferation efficacy of DOX-loaded FOE hydrogel (DOX-FOE) to mouse breast cancer (4T1) cells was compared with those of free DOX. The cell viability decreased gradually with increasing DOX concentration. It was found that the inhibitory efficacy of DOX-FOE surpassed that of free DOX (Fig. 3B). IC_{50} is a commonly used parameter to evaluate the cytotoxicity of preparations, and the lower the IC_{50} value, the better the proliferation inhibition effect of the preparation. The

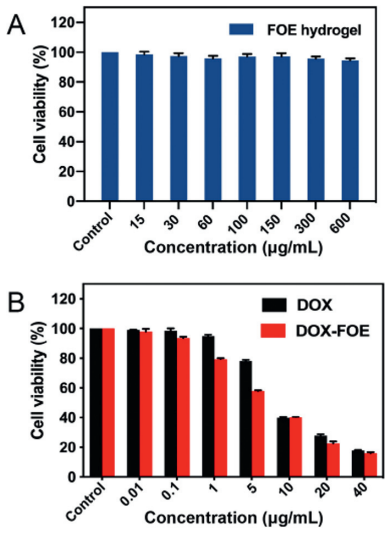

Fig. 3. (A) Cell viability of HUVECs co-incubated with FOE octapeptide hydrogel ($n = 6$); (B) Cell viability of 4T1 cells co-incubated with free DOX or DOX-loaded hydrogel ($n = 6$).

IC_{50} values of free DOX and DOX-FOE supported above observation, with 9.410 μg/mL in the DOX group and 5.625 μg/mL in the DOX-FOE group. The overall results indicated that DDS based on FOE hydrogel improved efficacy of hydrophobic drugs *in vitro* to a certain extent. The reasons may be that: (1) Nanofibers were internalized by cells, thus increasing the cellular uptake of DOX adsorbed on the surface of nanofibers [30,31]; (2) Compared with the passive diffusion of free DOX, the FOE hydrogel disintegrated under acidic conditions, resulting in the encapsulation of DOX in spherical nanogels, in which the endocytosis of nanospheres enhanced the cellular uptake of DOX [32,33]; (3) In the tumor microenvironment, the octapeptide exhibited a positive charge which attracted the negative charge of the cell membrane to reinforce the ability of cancer cells to absorb the octapeptide [34].

Next, we assessed the anti-tumor efficacy of DOX-FOE *in vivo*. All animal experiments herein were approved by the Ethics Committee of China Pharmaceutical University (Nanjing, China) and carried out specifically in accordance with guidelines evaluated and approved by this Committee. The changes of tumor volume and body weight of tumor-bearing mice after peritumoral administration of normal saline (NS), DOX and DOX-FOE were monitored to evaluate toxicity and tumor growth inhibition of the formulations (Figs. 4A and B). Compared to the significant growth of tumor volume for the NS-treated mice, the tumor volume in DOX group showed a slower growth to 328.01 mm^3, and that in DOX-FOE group remained relatively stable (167.07 mm^3) within 7 days. The results clearly meant that the tumor inhibitory effect of DOX-FOE was more obvious than that of free DOX ($P < 0.05$). Additionally, the mice in NS group showed an obvious increase in body weight after peritumoral administration (Fig. 4B). However, the change of body weight of the mice in DOX-FOE and DOX groups showed a downward trend. The average body weight of mice in DOX-FOE group decreased from 18.63 g to 18.26 g within 7 days, while that of mice in DOX group showed a significant decreased from 19.08 g to 17.17 g, suggesting that the toxicity of DOX was markedly reduced after being wrapped in FOE hydrogel. The reason may be that small molecular anticancer drugs cannot be selectively concentrated in tumor cells, whereas the drug-loaded hydrogel forms a "drug repository" around the tumor, which can target and release the drug continuously and slowly, thereby reducing the toxicity and side effects.

Figs. 4C and D showed the average weight and photographs of the excised tumors. The tumor weights of tumor-bearing mice in NS, DOX and DOX-FOE groups were 1.62 ± 0.26, 1.01 ± 0.11 and 0.64 ± 0.06 g, respectively. Compared with the DOX group, the anti-tumor effect of DOX-FOE group was more obvious, indicating that drug-loaded FOE hydrogel can significantly prolong the effect of anti-tumor drugs, which is consistent with results of *in vitro* studies. The results of hematoxylin and eosin (H&E) staining and TdT-mediated dUTP nick-end labeling (TUNEL) assay of tumor sections were shown in Fig. 4E. There were almost no obvious necrotic areas in the tumor tissue of NS group. In contrast, apparent necrotic areas were observed in DOX and DOX-FOE groups, and the necrotic areas in DOX-FOE group were more widely distributed. TUNEL assay results showed that the brown area in DOX-FOE group was larger compared with the NS and DOX group, indicating a greater degree of tumor tissues apoptosis in the hydrogel group, which supports the above results that DOX-FOE has good anti-tumor properties.

The distribution of DOX in mice was observed by *in vivo* imaging system using DiR fluorescent probe instead of DOX. The flu-

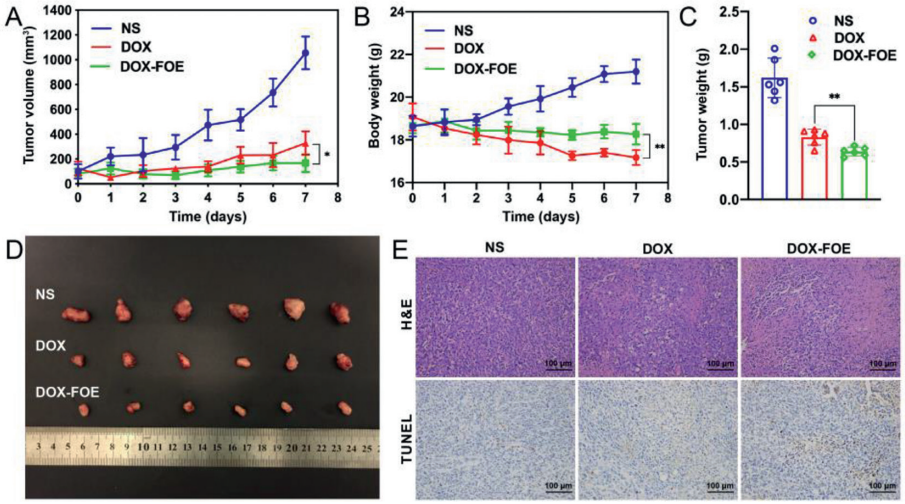

Fig. 4. *In vivo* anti-tumor assay of FOE hydrogel. Tumor volume (A) and body weight (B) change curve of 4T1 tumor-bearing BALB/c mice treated with NS, DOX and DOX-FOE within 7 days; Average weight (C) and photographs (D) of tumors harvested from 4T1 tumor-bearing BALB/c mice treated with NS, DOX and DOX-FOE 7 days after administration; (E) H&E staining and TUNEL assay of tumor sections harvested from 4T1 tumor-bearing BALB/c mice at 7 days posttreatment, scale bar: 100 μm. One-way ANOVA, mean ± SD, $^{*}P < 0.05$, $^{**}P < 0.01$ *versus* DOX.

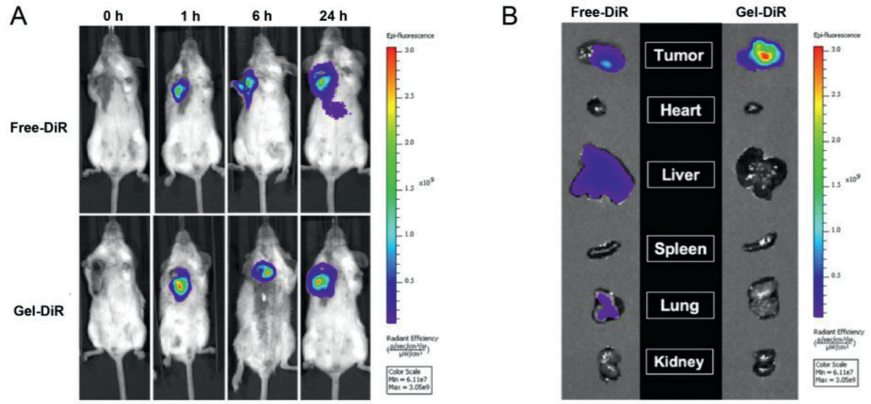

Fig. 5. *In vivo* biodistribution of free-DiR and Gel-DiR in 4T1-bearing mice. (A) *In vivo* fluorescence images of tumor-bearing mice at different times after peritumoral administration of free-DiR and Gel-DiR; (B) *Ex vivo* fluorescence images of tumors and major organs at 24 h after peritumoral administration, including tumor, heart, liver, spleen, lung, and kidney. DiR as the fluorescent probe.

orescence of DiR was significantly localized around the tumor in DiR-loaded FOE hydrogel (Gel-DiR) group at different time points (0, 1, 6, and 24 h) (Fig. 5A). However, in free DiR group, the fluorescence signal of the tumor site gradually weakened after 6 h, while the signal of other tissues enhanced. Likewise, significant signal appeared in the liver and lung of free DiR group after 24 h (Fig. 5B). On the contrary, in the Gel-DiR group, signal was still enriched in the tumor site, and there was no obvious signal in other organs, demonstrating that DOX-FOE could effectively prolong the action time of DOX and enhance drug accumulation at the tumor site, thereby reducing the side effects.

In summary, in order to overcome the challenges of hydrophobic chemotherapy drugs delivery, we designed and synthesized an injectable pH-sensitive ionic-complementary octapeptide FOE that could self-assemble to form hydrogel at pH 7.4 as a novel drug carrier. Especially, under acidic conditions, the pH-induced change of the secondary structure in the octapeptide led to the morphological transformation from nanofibers to nanospheres, which contributed to the achievement of controlled drug delivery and enhanced drug uptake by tumor cells. Besides, FOE hydrogel-based drug delivery system can be administered locally due to its satisfactory mechanical strength, fluidity and viscoelastic, so as to concentrate the anticancer drugs at the tumor site and reduce systemic adverse effects. In addition to economic advantage owing to the short and simple sequence, the octapeptide designed herein also has a broad prospect in the clinical application of drug delivery.

Declaration of competing interest

The authors declare that they have no known competing financial interests or personal relationships that could have appeared to influence the work reported in this paper.

Acknowledgments

This study was supported by the National Natural Science Foundation of China (Nos. 81572978 and 81760638), Special Science and Frontier Technology Research Project of Chongqing (No. cstc2016jcyjA0520), Innovative Technology in Military and Clinical Medicine (No. 2018JSLC0035), and Natural Science Foundation of Xinjiang Province (No. 2017D01C200).

Supplementary materials

Supplementary material associated with this article can be found, in the online version, at doi:10.1016/j.cclet.2021.10.058.

References

[1] J.A. Kemp, M.S. Shim, C.Y. Heo, Y.J. Kwon, Adv. Drug Deliv. Rev. 98 (2016) 3–18.
[2] C. Wu, J. Liu, X. Tang, et al., Chem. Commun. 55 (2019) 14852–14855.
[3] Y. Zhu, L. Wang, Y. Li, et al., Biomater. Sci. 8 (2020) 5415–5426.
[4] J. Huang, X. You, P. Xin, et al., Chin. Chem. Lett. 32 (2021) 1737–1742.
[5] M. Cagel, E. Grotz, E. Bernabeu, M.A. Moretton, D.A. Chiappetta, Drug Discov. Today 22 (2017) 270–281.
[6] N. Oliva, J. Conde, K. Wang, N. Artzi, Acc. Chem. Res. 50 (2017) 669–679.
[7] J. Xie, Y. Lu, B. Yu, J. Wu, J. Liu, Chin. Chem. Lett. 31 (2020) 1173–1177.
[8] A.S. Hoffman, Adv. Drug Deliv. Rev. 54 (2002) 3–12.
[9] Q. Huang, Y. Zou, M.C. Arno, et al., Chem. Soc. Rev. 46 (2017) 6255–6275.
[10] Y. Wen, J.H. Collier, Curr. Opin. Immunol. 35 (2015) 73–79.
[11] M. Norouzi, B. Nazari, D.W. Miller, Drug Discov. Today 21 (2016) 1835–1849.
[12] T. Thambi, Y. Li, D.S. Lee, J. Control. Release 267 (2017) 57–66.
[13] A.M. Jonker, D.W.P.M. Löwik, J.C.M. van Hest, Chem. Mater. 24 (2012) 759–773.
[14] J. Wang, K. Liu, R. Xing, X. Yan, Chem. Soc. Rev. 45 (2016) 5589–5604.
[15] X.R. You, L.Y. Wang, L. Wang, J. Wu, Adv. Funct. Mater. 31 (2021) 2100805.
[16] A. Mujeeb, A.F. Miller, A. Saiani, J.E. Gough, Acta Biomater. 9 (2013) 4609–4617.
[17] S. Eskandari, T. Guerin, I. Toth, R.J. Stephenson, Adv. Drug Deliv. Rev. 110-111 (2017) 169–187.
[18] M.J. Sis, M.J. Webber, Trends Pharmacol. Sci. 40 (2019) 747–762.
[19] F. Gelain, Z. Luo, S. Zhang, Chem. Rev. 120 (2020) 13434–13460.
[20] M.J. Webber, C.J. Newcomb, R. Bitton, S.I. Stupp, Soft Matter 7 (2011) 9665–9672.
[21] P. Liang, J. Zheng, S. Dai, et al., J. Control. Release 260 (2017) 22–31.
[22] Z.Y. Sun, C.J. Song, C. Wang, Y.Q. Hu, J.H. Wu, Mol. Pharm. 17 (2020) 373–391.
[23] N.K. Singh, D.S. Lee, J. Control. Release 193 (2014) 214–227.
[24] H. Zhang, J. Park, Y. Jiang, K.A. Woodrow, Acta Biomater. 55 (2017) 183–193.
[25] M.R. Caplan, P.N. Moore, S.G. Zhang, R.D. Kamm, D.A. Lauffenburger, Biomacromolecules 1 (2000) 627–631.
[26] Z. Yang, H. Xu, X. Zhao, Adv. Sci. 7 (2020) 1903718.
[27] G. Fichman, E. Gazit, Acta Biomater 10 (2014) 1671–1682.
[28] L. Mei, S. He, Z. Liu, K. Xu, W. Zhong, Chem. Commun. 55 (2019) 4411–4414.
[29] X.D. Xu, C.S. Chen, B. Lu, et al., J. Phys. Chem. B 114 (2010) 2365–2372.
[30] E. Beniash, J.D. Hartgerink, H. Storrie, J.C. Stendahl, S.I. Stupp, Acta Biomater. 1 (2005) 387–397.
[31] R. Tian, J. Chen, R. Niu, Nanoscale 6 (2014) 3474–3482.
[32] H. Wang, C. Yang, L. Wang, et al., Chem. Commun. 47 (2011) 4439–4441.
[33] R. Bawa, S.Y. Fung, A. Shiozaki, et al., Nanomedicine 8 (2012) 647–654.
[34] D. Ciumac, H. Gong, X. Hu, J.R. Lu, J. Colloid Interface Sci. 537 (2019) 163–185.